Geometrical resonance in a driven symmetric bistable system subjected to strong or to weak damping

Ricardo Chacón*
Departamento de Electrónica e Ingeniería Electromecánica, Escuela de Ingenierías Industriales, Universidad de Extremadura, Apartado 382, 06 071 Badajoz, Spain
(Received 19 January 1996)

The response of a symmetric bistable system driven by a time-periodic rectangular force modeled by the Jacobian elliptic function sn is studied in two limiting situations: overdamping and weak damping. For the overdamping case, the appearance of responses with the same shape and period as the driving force is explained in terms of a *geometrical resonance* phenomenon. The distortion of the response under changes in the forcing period and shape is also considered. For weak damping, the reduction of homoclinic chaos as the driving shape approximates the geometrical resonance forcing shape is explained by means of Melnikov's analysis in the asymptotic case of infinite period driving. [S1063-651X(96)08912-X]

PACS number(s): 05.45.+b

I. INTRODUCTION

Resonance is a key concept throughout the physical sciences and engineering. From Galileo's initial discussion in 1638 [1] to applications in highly nonlinear oscillators, where the response to harmonic driving forces can be determined using various methods [2–6], the notion of resonance (nonlinear resonance) has been identified with how well the driving period T_d fits (a rational fraction of) a natural period T_o of the underlying conservative system. Indeed, nonlinear resonance arises [7] as the direct extension of the usual concept in the linear limiting case, where the resonance response is regarded as the largest response, to the nonlinear (general) case, where, on the contrary, the response to harmonic driving forces is typically small and complicated [8]. Recently, it has been proposed [9] that the so-called geometrical resonance (GR) should really be considered the natural, *fully nonlinear* extension of the usual concept. For systems with periodic motions, GR means that the amplitude, period, and wave form (shape) of the driving signal must suitably fit to *preserve* a previously chosen natural periodic response from the underlying conservative system, if dissipation is considered, or from an equivalent conservative system for driven Hamiltonian systems. In both cases, the GR condition is derived from a *local* energy conservation requirement [9].

In this work I first attempt to explain and extend some previous results, obtained numerically, by using the notion of GR. The system to be studied is an overdamped bistable model [10] subjected to an external periodic modulation

$$\frac{dx}{dt} = x - x^3 + F\ \mathrm{sn}(\omega t; m), \tag{1}$$

where $\mathrm{sn}(\omega t; m)$ is the Jacobian elliptic function of parameter m and period T [$\omega = \omega(m) \equiv 4K(m)/T$ with $K(m)$ the complete elliptic integral of the first kind [11]]. When $m = 0$, then $\mathrm{sn}(\omega t; m = 0) = \sin(\omega t)$, i.e., one recovers the limit case of harmonic forcing. In the other limit,

$$\mathrm{sn}(\omega t; m = 1) = \frac{4}{\pi} \sum_{n=0}^{\infty} \frac{1}{2n+1} \sin[(2n+1) 2\pi t/T], \tag{2}$$

i.e., one obtains the Fourier expansion of the *square wave* function of period T [12]. With T constant, only the forcing shape is varied by increasing m from 0 to 1, and there is thus a smooth transition from a sine function to a square wave. In Ref. [13], the corresponding forcing term in (1) was an approximation to a rectangular signal with amplitude F and period T, generated by a Fourier series with 20 odd harmonics. The authors found numerically that, for each value of T, there exists a corresponding amplitude $F^*(T)$ such that for $F < F^*$ the motion is essentially confined within the initial well, while for $F > F^*$ the system trajectories explore both wells, describing large-amplitude oscillations around the origin. Away from the critical line $F^*(T)$, the shape of the response coincides basically with that of the forcing, while near the critical line the output has a very distorted shape, though it is still periodic with the same period T. As will be shown, these results naturally arise from an analysis of the GR responses.

The second goal of this paper is to demonstrate, for the weak damping limiting case, that the stability of homoclinic chaos arising from the whole bistable system

$$\ddot{x} = x - x^3 - \delta \dot{x} + F\ \mathrm{sn}(\Omega \tau; m) \tag{2'}$$

[$\dot{x} \equiv dx/d\tau$, $0 < \delta$, $F \ll 1$, $\Omega = \Omega(m) \equiv 4K(m)/T$], as the driving shape is varied, is also explained in terms of GR.

The rest of the paper is organized as follows. Section II gives the results concerning the GR analysis of the bistable system (1), where the forcing term is initially taken to be an indefinite T-periodic function. Further, it is demonstrated that when the forcing is given by a square wave function the GR requirements are almost exactly satisfied and an *amplitude-response* curve is deduced that indicates that the bistable system should, near a certain GR, exhibit a jump phenomenon. In Sec. III, a numerical study illustrates the accuracy and scope of the theoretical derivations. Section IV is devoted to analyzing the decrease (in parameter space)

*Electronic address: rchacon@unex.es

of homoclinic chaos arising from the symmetric bistable system (namely, the two-well Duffing oscillator [3,5]), subjected to both weak damping and small-amplitude sn forcing [Eq. (2′)], when $m\to 1$ and $T\to\infty$. It is shown theoretically, by using Melnikov's method, that the mechanism underlying the regularization of the dynamics is the approximation to a GR solution. Finally, Sec. V includes a summary of the results and conclusions.

II. OVERDAMPING: GEOMETRICAL RESONANCE ANALYSIS

Without regard for any specific physical context at the outset, let us begin with the overdamped model

$$\frac{dx}{dt}=-U'(x)+Ff(t), \tag{3}$$

where $f(t)$ is an *a priori* arbitrary T-periodic function with unit amplitude and the prime refers to the derivative of the arbitrary potential $U(x)$. Observe that the precise characteristic of the GR, for a general system to be driven, is that of *preserving* a given natural response (whether periodic or not) of the unperturbed system. Now, with that in mind, let us consider the special (steady) solutions $x_s(t)$, with amplitude A, such that $x_s(t)=Af(t)$, i.e., when the external excitation and the response have both the same period (usual resonance) and the same shape, including when the natural responses are not periodic. Under this assumption, the dynamics is equivalent to that of a particle having total energy E given by

$$E=\tfrac{1}{2}\dot{x}_s^2+U_{\rm eq}(x_s)=\text{const}, \tag{4}$$

with

$$U_{\rm eq}(x_s)\equiv-\left[\frac{F}{A}x_s-U'(x_s)\right]^2 \tag{5}$$

the *equivalent potential* [14]. With $E\equiv 0$ (the system is overdamped) one directly obtains the solutions corresponding to the general model (3),

$$\int_{x_0}^{x}\frac{dx}{Fx/A-U'(x)}=t. \tag{6}$$

For the two-well potential [cf. Eq. (1)], the particular responses (6) are

$$x(t)=\begin{cases}\pm\sqrt{\dfrac{|\eta|}{2}}\left[\dfrac{x_0^2}{|\eta|+x_0^2}\right]^{1/4}e^{-|\eta|t/2}\,\operatorname{csch}^{1/2}\{|\eta|t-\tfrac{1}{2}\ln[x_0^2/(|\eta|+x_0^2)]\}, & \eta<0 \quad (7a)\\ \pm x_0[1+2x_0^2t]^{-1/2}, & \eta=0 \quad (7b)\\ \pm\sqrt{\dfrac{\eta}{2}}\left[\dfrac{x_0^2}{\eta-x_0^2}\right]^{1/4}e^{\eta t/2}\operatorname{sech}^{1/2}\{\eta t+\tfrac{1}{2}\ln[x_0^2/(\eta-x_0^2)]\}, & \eta>0, \quad (7c)\end{cases}$$

with $x(t=0)=\pm x_0$, and

$$\eta\equiv 1+\frac{F}{A}. \tag{8}$$

Observe that the asymptotic behavior is that of equilibrium states

$$\lim_{t\to\infty}x(t)\equiv x_s(t)=\begin{cases}0, & \eta\leqslant 0\\ \pm\sqrt{\eta}, & \eta>0,\end{cases} \tag{9}$$

which do not depend on the initial condition x_0. It is worth mentioning that the above scheme is similar to that employed in seeking traveling waves of permanent form (the so-called phase plane analysis [15]); indeed, from it one generally obtains an energylike equation [analogous to Eq. (4)] whose physical solutions, representing stationary waves, are discussed qualitatively in Ref. [15] for different values of the energylike quantity (constant of integration). Thus one finds that the solution (7c) is similar to kink solutions arising from the sine-Gordon equation (cf. Ref. [15]), for example.

Note that $\eta=\eta_c\equiv 0$ is the critical value for the topological change (*symmetry breaking*) in the shape of the corresponding equivalent potential [cf. Eq. (5)]. Therefore, one would suppose that a rectangular forcing would satisfy, *intermittently over time*, the requirements of a GR if $F/A+1>0$. Indeed, let us assume that $x_s(t)=A\ \text{sn}(\omega t;m)$ is an intermittent-GR solution, i.e., that it should verify

$$\frac{dx_s}{dt}=\eta x_s-x_s^3. \tag{10}$$

Using Ref. [11], one straightforwardly obtains

$$\frac{dx_s}{dt}=[4AK(m)/T]\,\text{cn}(\omega t;m)\,\text{dn}(\omega t;m), \tag{11}$$

$$\eta x_s-x_s^3=A[\eta-A^2\text{sn}^2(\omega t;m)]\,\text{sn}(\omega t;m), \tag{12}$$

where $\text{cn}(\omega t;m)$ and $\text{dn}(\omega t;m)$ are the Jacobian elliptic functions [11] of parameter m. Now, it is possible to rewrite (11) in the form

$$\frac{dx_s}{dt}=A\left(\frac{2\pi}{T}\right)D^*(t;T,m)\,\text{dn}(4Kt/T;m)$$
$$=A\left(\frac{2\pi}{T}\right)D(t;T/2,m)\,\text{cn}(4Kt/T;m), \tag{13}$$

with

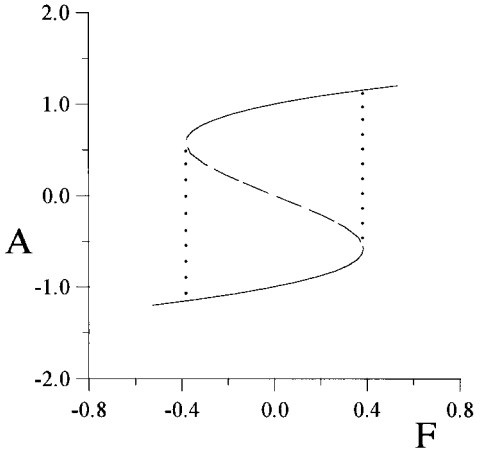

FIG. 1. Amplitude-response curve [Eq. (17)] for a rectangular forcing at geometrical resonance (see the text). The dashed line indicates an unstable response. F and A are in arbitrary length units.

$$D^*(t;T,m)\equiv\frac{2K}{\pi}\mathrm{cn}(4Kt/T;m), \tag{14a}$$

$$D(t;T,m)\equiv\frac{2K}{\pi}\mathrm{dn}(2Kt/T;m). \tag{14b}$$

These functions have the remarkable properties

$$D^*(t;T,m=0)=\cos(2\pi t/T), \tag{15a}$$

$$D^*(t;T,m=1)=\delta_{1,s}(t;T/2), \tag{15b}$$

$$D(t;T,m=0)=1, \tag{15c}$$

$$D(t;T,m=1)=\delta_{1,a}(t;T), \tag{15d}$$

where $\delta_{1,s}(t;T/2)$ [$\delta_{1,a}(t;T)$] is the symmetrical (asymmetrical) periodic δ function of period $T/2$ (T), i.e., they provide *nonideal* representations of periodic sequences of pulses. Now, taking the limit $m\to 1$, we see that the right-hand side (rhs) of (13) vanishes on a set of points that has Lebesgue measure zero [16]. This is also the case for the rhs of (12) if we set

$$\eta=A^2. \tag{16}$$

Therefore, a square-wave function of certain amplitude A^* (see below) is an intermittent-GR response to (1) if the following cubic equation is satisfied [cf. Eqs. (8) and (16)]:

$$A^3-A-F=0. \tag{17}$$

Its solution provides the amplitude-response curve for the *a priori* possible intermittent-GR responses and is illustrated in Fig. 1. The expected solutions $x_s(t)=A^*\mathrm{sn}(\omega t;m=1)$ will be observed only if they are stable, i.e., if any small perturbation δx of x_s is damped. Writing $x=x_s+\delta x$, for $\delta x\ll 1$ one gets (to first order)

$$\frac{d(\delta x)}{dt}=[1-3\eta\ \mathrm{sn}^2(\omega t;m=1)]\delta x, \tag{18}$$

with solutions [16]

$$\delta x(t)=\delta x(0)e^{(1-3\eta)t}. \tag{19}$$

Therefore, the above intermittent-GR responses will be observed if and only if $A+3F/2>0$ [cf. Eq. (8)]. That $\mathrm{sgn}(A)\neq\mathrm{sgn}(F)$ means that the forcing and the rectangular response are phase shifted by 2K (i.e., $T/2$ in time). It is worth mentioning that over the range $F\in\,]-2\sqrt{3}/9,2\sqrt{3}/9[$ one can expect the amplitude A^* of the rectangular responses to be given by $A^*=(|A_{s,1}|-|A_{s,2}|)/2$, where $A_{s,1},A_{s,2}$ ($|A_{s,1}|>|A_{s,2}|$) are the predicted (stable) solutions from the amplitude-response relation [Eq. (17)]. This can be understood by noting that such solutions would represent stable pure GR responses [cf. Eqs. (9) and (16)]. Hence the expected response under rectangular driving will visit periodically those two equilibrium states. On the other hand, for $|F|>2\sqrt{3}/9$, A^* will be given by the single solution of (17), which may be understood as the orbit exploring both wells, describing large amplitude oscillations around the origin. The amplitude-response curve shown in Fig. 1 indicates that the bistable system (1) subjected to a rectangular forcing ($m=1$) should (at GR) exhibit a discontinuous transition between the two above-mentioned periodic behaviors when F is varied slowly. This discontinuous jumping between the two stable (interior and exterior) orbits is a consequence of the nonlinear amplitude-response relation [Eq. (17)].

III. NUMERICAL RESULTS

The differential system (1) was integrated by using a fourth-order Runge-Kutta method with time steps chosen in the range $\Delta t=0.001$–0.005. In most of the numerical experiments the rectangular forcing was approximated by the $\mathrm{sn}(4Kt/T;m)$ driver with $m=1-10^{-15}$, which was sufficient for the present purposes (see Fig. 2). For T large enough and $m=1-10^{-15}$, the shape and period of the response coincide very closely with those of the driving, i.e., it is an intermittent-GR response. It is interesting to study the stability of such responses under changes in the forcing period. Figure 3 gives the time series of the displacement for increasing values of T. The associated limit cycles are plotted in Fig. 4. In all cases, response and driving have the same period (usual resonance). Observe that the intermittent-GR response is approached as T increases. These numerical results are in agreement with the theoretical discussion of Sec. II [cf. Eqs. (12) and (13)]. Indeed, as $\mathrm{sn}(4Kt/T;m=1-10^{-15})$ is not exactly a square-wave function [cf. Eq. (2)],

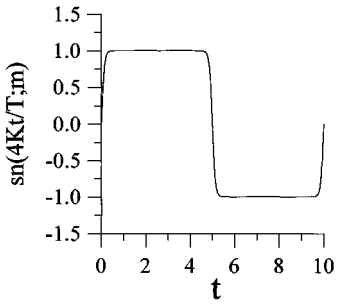

FIG. 2. Function $\mathrm{sn}(4Kt/T;m)$ vs t for $T=10$ and $m=1-10^{15}$; t is a dimensionless variable.

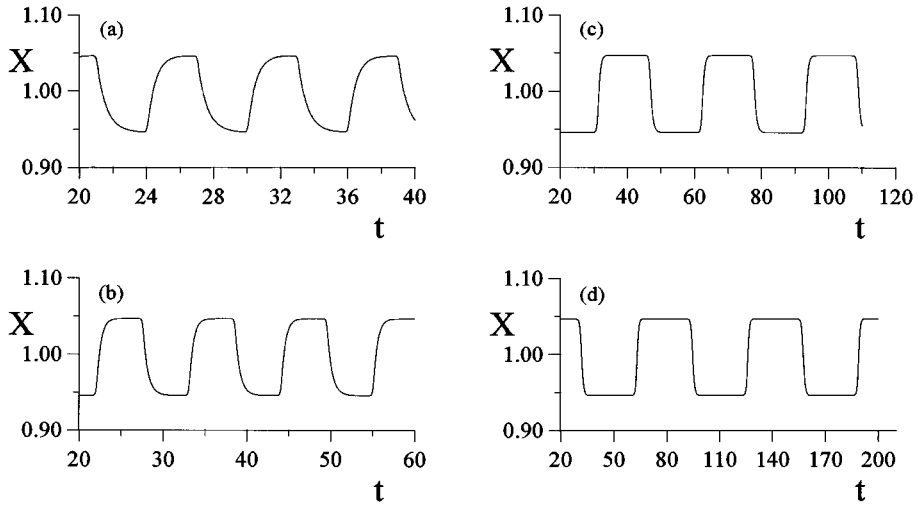

FIG. 3. Displacement time series for $F=0.1$ and $m=1-10^{-15}$; t is a dimensionless variable and x is in arbitrary length units. (a) $T=6$, (b) $T=11$, (c) $T=31$, and (d) $T=20\pi$.

the difference over time between (12) and (13) is no longer only on a set that has Lebesgue measure zero, but the value of such a difference (at each instant t) decreases as $1/T\rightarrow 0$, i.e., as the GR requirement is approached. Another way to approach an intermittent-GR response involves fixing the period and changing the forcing shape. Figure 5 shows three time series of the velocity for increasing values of m. The corresponding limit cycles are plotted in Fig. 6. As the forcing amplitude is relatively small ($F=0.1$), the orbits are confined to the initial well, near the bottom. Hence the system presents a quasi-GR for a wide range of forcing shapes (Fig. 5). The approach to the exact intermittent-GR is characterized by an increase in the velocity amplitude, while the displacement amplitude remains constant (see Fig. 6) as $m\rightarrow 1$. However, the temporal interval in which the velocity amplitude is negligible increases as $m\rightarrow 1$. For $F=0.1$ the amplitude-response relation (17) has the roots $A_{\mathrm{I}}=1.046\,68$, $A_{\mathrm{II}}=0.9456$, and $A_{\mathrm{III}}=-0.101\,031$, and it is found numerically that $A^{*}\simeq(A_{\mathrm{I}}+A_{\mathrm{II}})/2$ for all m values considered, as expected from the discussion in Sec. II. Therefore, when there is a confinement of the dynamics to close to the bottom of one well ($F\ll 1$), we can estimate analytically the average energy of the orbit as a function of both m and T,

$$\langle\mathcal{E}\rangle\equiv\frac{1}{T}\int_0^T\{\tfrac{1}{2}\dot{x}^2(t)+U[x(t)]\}dt, \tag{20}$$

with $U(x)=-x^2/2+x^4/4$ and $x(t)=A^{*}\mathrm{sn}(4Kt/T;m)$. After some simple algebraic manipulation, Eq. (20) can be recast into the form

$$\langle\mathcal{E}\rangle=\frac{1}{4K}\left\{2K\left(\frac{4KA^{*}}{T}\right)^2-\frac{A^{*2}}{2}\left[1+(1+m)\left(\frac{4K}{T}\right)^2\right]\times\int_0^{4K}\mathrm{sn}^2(\tau)d\tau+\frac{A^{*2}}{2}\left[m\left(\frac{4K}{T}\right)^2+\frac{A^{*2}}{2}\right]\times\int_0^{4K}\mathrm{sn}^4(\tau)d\tau\right\}. \tag{21}$$

The resulting integrals can be evaluated from standard tables [17]. Finally, we obtain

$$\langle\mathcal{E}\rangle=\frac{A^{*2}}{2}\left\{\left(\frac{4K}{T}\right)^2-4\left[1+(1+m)\left(\frac{4K}{T}\right)^2\right]\frac{(K-E)}{m}+\frac{4}{3m^2}[(2+m)K-2(1+m)E]\left[A^{*2}+m\left(\frac{4K}{T}\right)^2\right]\right\}, \tag{22}$$

where E is the complete elliptic integral of the second kind. For comparison with the pure GR responses (9), a plot of $\langle\mathcal{E}\rangle$ vs m, for $A^{*}=0.101\,08$ and $T=100$, is shown in Fig. 7. It is clear that the average energy diminishes as the intermittent-GR shape is approached (as expected), since the pure GR responses [Eq. (9)] are equilibrium states in this problem. Figure 8 illustrates the jumping phenomenon between the two rectangular (inner and outer) responses. The distortion of the response as F crosses the critical value $F_c=2\sqrt{3}/9$ is due to the forcing not being exactly a square-wave function ($m=1$) [Eq. (2)].

IV. WEAK DAMPING: GEOMETRICAL RESONANCE ANALYSIS

Let us study now the opposite limiting case—weak damping—by considering the perturbed two-well Duffing

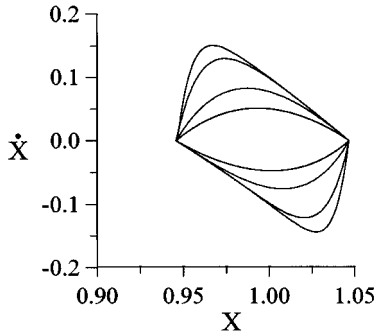

FIG. 4. Limit cycles corresponding to the time series in Fig. 3. The period decreases from the inner orbit ($T=20\pi$) to the external orbit ($T=6$). x and dx/dt are in arbitrary length units.

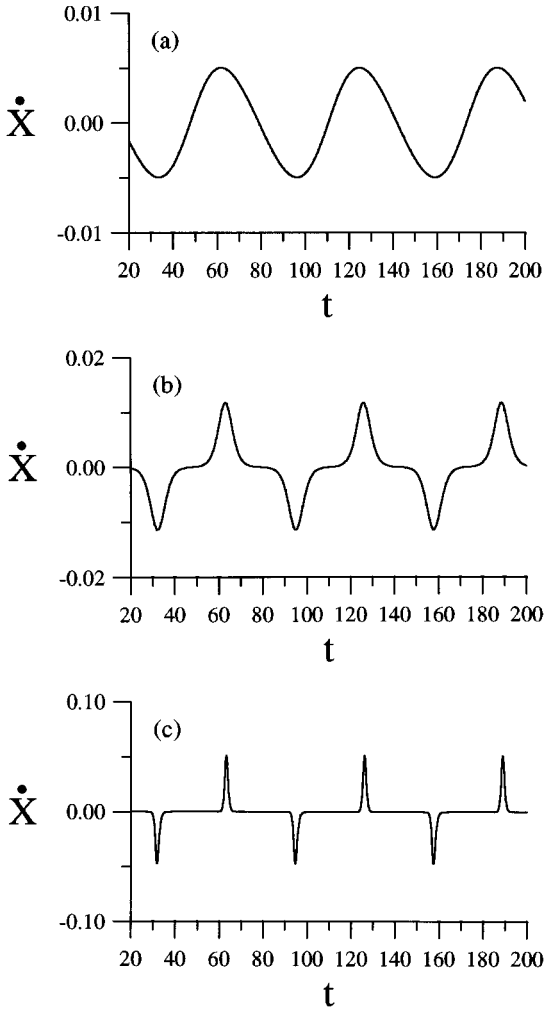

FIG. 5. Time series of the velocity for $T=20\pi$ and $F=0.1$. dx/dt is in arbitrary length units and t is a dimensionless variable. (a) $m=0$, (b) $m=0.99$, and (c) $m=1-10^{-15}$.

equation $(2')$. The application of Melnikov analysis (see, e.g., Refs. [5,6]) yields [12] the Melnikov distance

$$\Delta(\tau_0)=-\frac{4\delta}{3}\pm\frac{4F\pi^3}{\sqrt{2}}\sum_{n=0}^{\infty}a_n(m)b_n(T)\cos\left[\frac{(2n+1)2\pi\tau_0}{T}\right], \tag{23}$$

$$a_n(m)\equiv\operatorname{csch}\left[\left(n+\frac{1}{2}\right)\frac{\pi K'}{K}\right]\Big/(K\sqrt{m}), \tag{24}$$

$$b_n(T)\equiv(2n+1)\operatorname{sech}[(2n+1)\pi^2/T]/T, \tag{25}$$

with K' the complementary complete elliptic integral of the first kind [17]. From Eqs. (23)–(25), one can see that a homoclinic bifurcation, *signifying the onset of chaos*, is guaranteed for trajectories, the initial conditions of which are sufficiently near the unperturbed separatrix

$$x_{\rm sep}(\tau)=\pm\sqrt{2}\ \operatorname{sech}\tau,\quad \dot{x}_{\rm sep}(\tau)=\pm\sqrt{2}\ \operatorname{sech}\tau\tanh\tau \tag{26}$$

if

$$\delta/F<U(m,T), \tag{27}$$

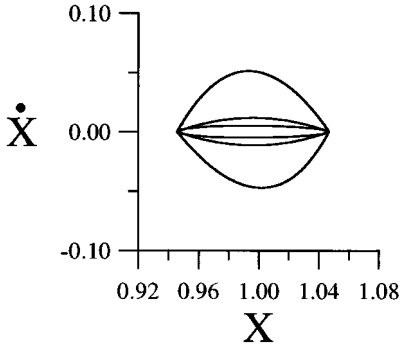

FIG. 6. Limit cycles corresponding to the time series in Fig. 5. The value of m increases from the inner orbit ($m=0$) to the external orbit ($m=1-10^{-15}$). x and dx/dt are in arbitrary length units.

where the threshold function is

$$U(m,T)\equiv\frac{3\sqrt{2}\pi^3}{2}\sum_{n=0}^{\infty}a_n(m)b_n(T). \tag{28}$$

The upper (lower) sign in (23) and (26) refers to the right (left) homoclinic orbit. For the limiting cases of harmonic [$\sin(\Omega\tau)=\mathrm{sn}(\Omega\tau;m=0)$] and square-wave [$m=1$, Eq. (2)] forcing, one obtains, respectively,

$$U(m=0,T)=\frac{3\pi^2\sqrt{2}}{2T}\operatorname{sech}\left(\frac{\pi^2}{T}\right), \tag{29}$$

$$U(m=1,T)=\frac{6\pi\sqrt{2}}{T}\sum_{n=0}^{\infty}\operatorname{sech}\left[\frac{(2n+1)\pi^2}{T}\right], \tag{30}$$

with

$$\lim_{T\to0}U(m=0,T)=\lim_{T\to0}U(m=1,T)=0. \tag{31}$$

Since, as is well known [18], Melnikov's method predictions are only valid for motions based at points sufficiently near the separatrix of the unperturbed system, we will here consider the GR concerning the separatrix (26) (i.e., special orbit with period $T_{\rm sep}=\infty$). First, therefore, we need to obtain the

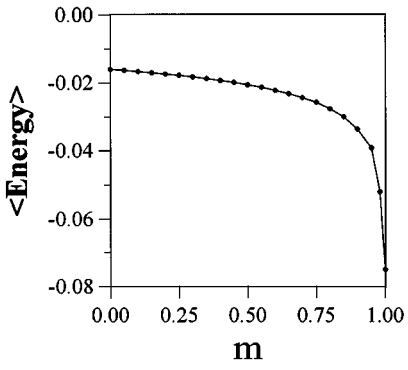

FIG. 7. Average energy of the response $\langle\mathcal{E}\rangle$ vs m [Eq. (22)] for $A^*=0.101\,08$ and $T=100$. $\langle\mathcal{E}\rangle$ is in arbitrary squared length units and m is a dimensionless variable. The points represent actual results and are connected by lines to guide the eye.

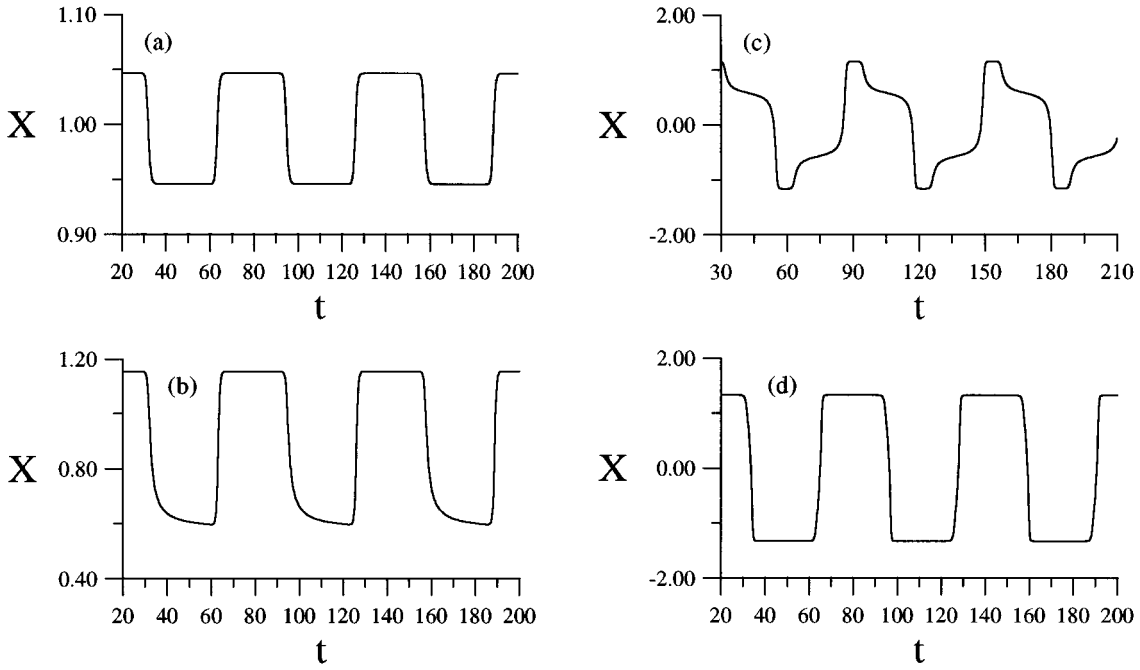

FIG. 8. Time series of the displacement for $T=20\pi$ and $m=1-10^{-15}$. x is in arbitrary length units and t is a dimensionless variable. (a) $F=0.1$, (b) $F=2\sqrt{3}/9$, (c) $F=0.395$, and (d) $F=1$.

limits of the threshold functions (29) and (30) when $T\to\infty$. To this end, note that (30) can be rewritten [19]

$$U(m=1,T)=\frac{3\sqrt{2}}{2}\left[1+2\sum_{n=1}^{\infty}(-1)^n\operatorname{sech}\left(\frac{nT}{2}\right)\right] \quad (32)$$

and then [cf. Eqs. (29) and (32), respectively]

$$\lim_{T\to\infty} U(m=0,T)=0, \quad (33)$$

$$\lim_{T\to\infty} U(m=1,T)=3\frac{\sqrt{2}}{2}. \quad (34)$$

Equation (33) implies that in this limit chaotic behavior is not possible because the harmonic forcing tends to zero.

Second, note that the forcing corresponding to a GR for the separatrix (26) (i.e., the forcing permitting the survival of this separatrix [9]) is written

$$F_{\mathrm{RG,sep}}(\tau)=\mp\sqrt{2}\delta\ \operatorname{sech}\tau\ \tanh\tau, \quad (35)$$

which cannot be recovered from $F\ \mathrm{sn}[4K\tau/T;m]$ for any value of the parameters m,T. However, we can require the sn forcing to be resonant (period) with either the interior or exterior orbits of the unperturbed two-well Duffing oscillator and then take the limit $T\to\infty$ to see how well the GR forcing (35) is approximated depending on the shape of the resulting functions. In this way, we will test the exclusive characteristic of the GR (shape) by calculating the corresponding threshold functions [cf. Eq. (27)]. The periods of the orbits inside and outside the homoclinic orbits (26) are [18], respectively,

$$T^{\mathrm{in}}(m)=2K(m)\sqrt{2-m}, \quad (36)$$

$$T^{\mathrm{out}}(m)=4K(m)\sqrt{2m-1}. \quad (37)$$

It is obvious that $T^{\mathrm{in,out}}(m\to1)\to\infty$. Therefore, we obtain

$$\lim_{m\to1}\ \mathrm{sn}[4K\tau/T^{\mathrm{in}};m]=\tanh(2\tau), \quad (38)$$

$$\lim_{m\to1}\ \mathrm{sn}[4K\tau/T^{\mathrm{out}};m]=\tanh(\tau). \quad (39)$$

It is straightforward to calculate [20] the associated threshold functions [cf. Eq. (27)] to the limiting cases (38) and (39):

$$U^{\mathrm{in}}(m\to1,T=T^{\mathrm{in}})=\frac{3\pi}{2}(\sqrt{2}-1), \quad (40)$$

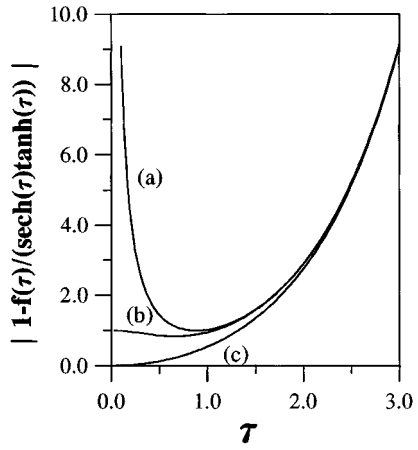

FIG. 9. Function $|1-f(\tau)/\operatorname{sech}\tau\ \tanh\tau|$ vs τ (τ is a dimensionless variable) for (a) $f(\tau)=\lim_{T\to\infty}\mathrm{sgn}[\sin(2\pi\tau/T)]$ [cf. Eq. (2)], (b) $f(\tau)=\tanh(2\tau)$ [Eq. (38)], and (c) $f(\tau)=\tanh\tau$ [Eq. (39)].

$$U^{\text{out}}(m\to 1, T=T^{\text{out}})=\frac{3\sqrt{2}}{2}\left(\frac{\pi}{4}\right). \tag{41}$$

By comparing now Eq. (34) with Eqs. (40) and (41) one finds $U^{\text{SW}}>U^{\text{in}}>U^{\text{out}}$, i.e., the range of δ/F for the onset of chaos is broader for the square wave out of resonance (period) than for the inner orbit resonant case, which, in turn, is broader than the exterior case. As all these results are obtained for $T=\infty$, one expects that they could be explained in terms of how near or far the shape (of the limiting forcings) is from the GR forcing shape. This is shown in Fig. 9, where the relative difference $|1-f(\tau)/\text{sech}\tau\,\tanh\tau|$ vs τ for the functions $f(\tau)=\{\lim_{T\to\infty}\text{sgn}[\sin(2\pi\tau/T)],\ \tanh(2\tau),\ \tanh(\tau)\}$ [cf. Eqs. (2), (38), and (39), respectively] is plotted. Note that the consequences deriving from the plots are in complete agreement with the above threshold function relationship, i.e., the closer the GR forcing shape is approached, the narrower the range of δ/F for the onset of chaos.

V. CONCLUSION

In this paper, first, I have investigated the stability of the responses of an overdamped bistable system under a periodic forcing of rectangular shape. The analysis shows that the preservation of responses with the same period and shape as the forcing is a consequence of a GR phenomenon. A jump phenomenon was derived theoretically, characterizing the discontinuous transition between GR motion confined within a well and GR motion around the two wells. In addition, for motion near the bottom of a well, an analytical expression was obtained for the average energy of the GR orbits, indicating that this energy decreases as $m\to 1$, i.e., as the square-wave shape is approached. Numerical experiments confirmed all the theoretical results. Second, for the weak damping case, there was shown to be a reduction (in parameter space) of homoclinic chaos as the driving shape approaches the GR forcing shape. It is thus clear that the GR concept provides a powerful tool with which to investigate the dynamics arising from a nonlinearly driven system where the usual (period) resonance analysis seems to be powerless.

[1] *Opere de Galileo Galilei*, edited by A. Favaro (Barbèra, Firenze, 1909).

[2] N. Minorsky, *Nonlinear Oscillations* (Krieger, Malabar, FL, 1962), p. 356.

[3] A. H. Nayfeh and D. T. Mook, *Nonlinear Oscillations* (Wiley, New York, 1979), p. 161.

[4] J. Kevorkian and J. D. Cole, *Perturbation Methods in Applied Mathematics* (Springer-Verlag, New York, 1981), p. 141.

[5] J. Guckenheimer and P. J. Holmes, *Nonlinear Oscillations, Dynamical Systems, and Bifurcations of Vector Fields* (Springer, New York, 1983), p. 171.

[6] A. J. Lichtenberg and M. A. Lieberman, *Regular and Stochastic Motion* (Springer, New York, 1983), p. 100.

[7] See, e.g., N. Minorsky, *Nonlinear Oscillations* (Ref. [2]), p. 236; A. J. Lichtenberg and M. A. Lieberman, *Regular and Stochastic Motion* (Ref. [6]), p. 70.

[8] See, e.g., *Chaotic Oscillations*, edited by T. Kapitaniak (World Scientific, Singapore, 1992).

[9] R. Chacón, Phys. Rev. Lett. **77**, 482 (1996).

[10] See, e.g., H. Haken, *Synergetics. An Introduction* (Springer-Verlag, Berlin, 1983), and references therein.

[11] L. M. Milne-Thomson, in *Handbook of Mathematical Functions*, edited by M. Abramowitz and I. A. Stegun (Dover, New York, 1972).

[12] R. Chacón and J. Díaz Bejarano, Phys. Rev. Lett. **71**, 3103 (1993).

[13] M. Morillo and J. Gómez-Ordóñez, Phys. Rev. E **51**, 999 (1995).

[14] Note that the energy conservation requirement can also be satisfied for a more general choice: $f(t)=(1/A)g[x_s(t)]$. But away from the linear case, the resonance (period) requirement generally is not verified.

[15] See, e.g., P. G. Drazin and R. S. Johnson, *Solitons: An Introduction* (Cambridge University Press, Cambridge, 1989); E. Infeld and G. Rowlands, *Nonlinear Waves, Solitons and Chaos* (Cambridge University Press, Cambridge, 1990).

[16] Sets that have Lebesgue measure zero are negligible for integration. See, e.g., W. Rudin, *Principles of Mathematical Analysis* (McGraw-Hill, New York, 1964), p. 343.

[17] P. D. Byrd and M. D. Friedman, *Handbook of Elliptic Integrals for Engineers and Scientists* (Springer, Berlin, 1971), pp. 191 and 192.

[18] S. Wiggins, *Introduction to Applied Nonlinear Dynamical Systems and Chaos*, Texts in Applied Mathematics Vol. 2 (Springer-Verlag, New York, 1990).

[19] A. T. Pérez (private communication).

[20] R. Chacón (unpublished).